

High-Resolution Probes of Low-Resolution Nuclei

R. J. Furnstahl

Department of Physics, Ohio State University, Columbus, OH 43085

Abstract

Renormalization group (RG) methods used to soften Hamiltonians allow large-scale computational resources to be used to greater advantage in calculations of nuclear structure and reactions. These RG transformations lower the effective resolution of the nuclei, which raises questions about how to calculate and interpret high-momentum transfer probes of nuclear structure. Such experiments are conventionally explained in terms of short-range correlations, but these disappear with the evolution to low-momentum scales. We highlight the important issues and prospects in the context of recent developments in RG technology, with guidance from the analogous extraction of parton distributions.

Keywords: *Renormalization group; nuclear structure*

1 Introduction

Recent electron scattering experiments on nuclei that use large four-momentum transfers to knock out nucleons have been interpreted in terms of short-range correlations (SRCs) in the nuclear wave function [1, 2]. As indicated schematically in Fig. 1 (top), the dominant source of ejected back-to-back nucleons is identified as the break-up of an SRC formed by low-momentum nucleons being coupled to high-momentum by the nucleon-nucleon (NN) interaction. At the same time, the use of softened (“low-momentum”) Hamiltonians has had great success in pushing the limits of microscopic calculations of nuclear structure and reactions [3–5]. This success is in large part due to the *absence* of SRCs in the corresponding nuclear wave functions. We seek to reconcile these results by applying a renormalization group (RG) viewpoint, which manifests the scale (and scheme) dependence of nuclear Hamiltonians and operators by continuous changes in the *resolution*. RG transformations shift the physics between structure and reaction mechanism so that the same data can have apparently different explanations. We use the RG perspective to discuss implications in light of the current and future possibilities of applying new RG technology.

The RG is a powerful and versatile tool for this purpose. The common features of the RG for critical phenomena and high-energy scattering are discussed by Steven Weinberg in an essay in Ref. [6]. He summarizes:

“The method in its most general form can I think be understood as a way to arrange in various theories that the degrees of freedom that you’re talking about are the relevant degrees of freedom for the problem at hand.”

This is the essence of what we do by evolving to low-momentum interactions: we arrange for the degrees of freedom to be the relevant ones for nuclear structure (and reactions). This does not mean that other degrees of freedom cannot be used (including SRCs from high-momentum interactions), but we need to be mindful of Weinberg’s

Proceedings of International Conference ‘Nuclear Theory in the Supercomputing Era — 2013’ (NTSE-2013), Ames, IA, USA, May 13–17, 2013. Eds. A. M. Shirokov and A. I. Mazur. Pacific National University, Khabarovsk, Russia, 2014, p. 371.
<http://www.ntse-2013.khb.ru/Proc/Furnstahl.pdf>.

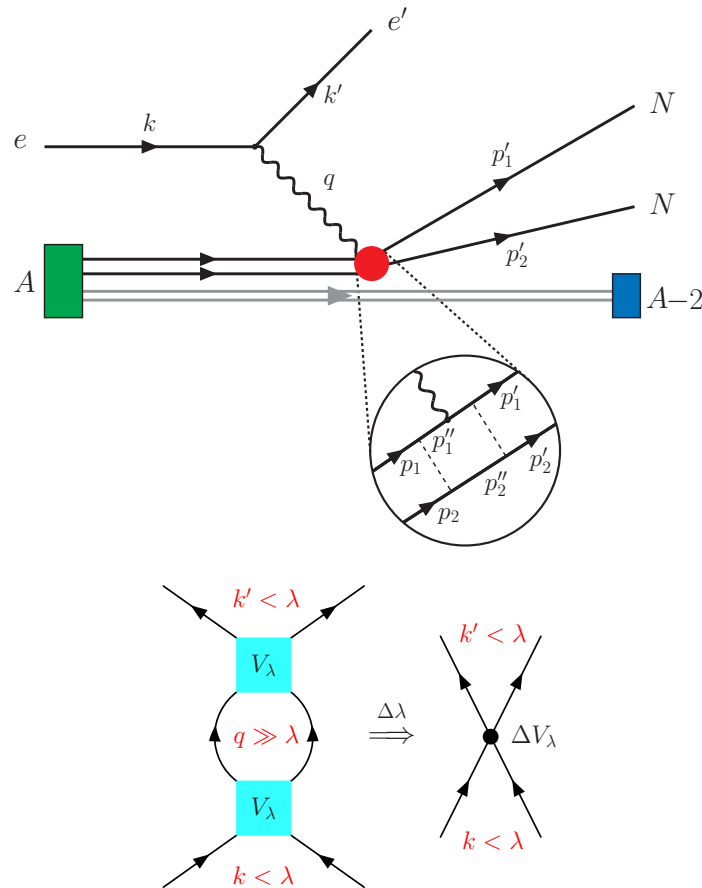


Figure 1: Schematic two-nucleon knock-out experiment with SRC interpretation (top) and diagrammatic illustration that the contribution of decoupled high-momentum modes in intermediate states is replaced by (regularized) contact interactions (bottom).

adage [6]:

“You can use any degrees of freedom you want, but if you use the wrong ones, you’ll be sorry.”

The benefits of applying RG to high-energy (particle) physics include improving perturbation theory, e. g., in QCD. A mismatch of energy scales can generate large logarithms that ruins perturbative convergence even when couplings by themselves are small. The RG shifts strength between loop integrals and coupling constants to reduce these logs. For critical phenomena in condensed matter systems, the RG reveals the nature of observed universal behavior by filtering out short-distance degrees of freedom.

Both these aspects are seen in applications of RG to nuclear structure and reactions. As the resolution is lowered, nuclear calculations become more perturbative, implying that scales are more appropriately matched. In addition, the potentials flow toward universal form (e. g., see Fig. 3) as model dependent short-distance details are suppressed. The end result might be said to make nuclear physics look more like quantum chemistry computationally, opening the door to a wider variety of techniques (such as many-body perturbation theory) and simplifying calculations (e. g., by improving convergence of basis expansions). However, maintaining RG-induced three-nucleon (NNN) forces (and possibly four-nucleon forces) has been found to be essential for

accurate and scale-independent results. Recently developed RG technology to handle three-body evolution [4, 7, 8] will be critical to realize the power of the RG.

2 Similarity renormalization group flow

Renormalization group methods and applications to nuclear systems are well documented in the literature (see Refs. [3, 5] and references therein) and in contributions to these proceedings. A popular approach, which we focus on here, is the similarity renormalization group (SRG). In most implementations of the SRG, an initial Hamiltonian (typically with both NN and NNN interactions) is driven by a series of continuous unitary transformations toward more diagonal form in momentum representation. This flow toward the diagonal is illustrated for both NN and NNN matrix elements in Fig. 2 [8]. More diagonal means greater decoupling of low- and high-momentum modes, making interactions more perturbative. The changes in many-body interactions highlight the need to be able to control this part of the evolution.

Where does the physics of the decoupled high-momentum modes go? It flows to modifications of the low-momentum parts of both the two- and three-nucleon interactions, which effective field theory (EFT) tells us can be absorbed into regulated contact interactions (as indicated schematically in the bottom in Fig. 1). That the leading change in the NN potential induced by the SRG does have this form can be shown using the operator product expansion (see Section 3 and Refs. [10, 11]) but it is implicit in the NN 1S_0 partial wave in Fig. 3, where the off-diagonal matrix elements of a set of chiral EFT NN potentials with different regularization schemes (left) are evolved to low resolution (right). We directly see the suppression of off-diagonal strength for $k > \lambda$ and a flow to universal values when the high-momentum model dependence is suppressed (evidence for universal flow has also been observed in three-body evolution [7, 8]). The dominant change in the potential at low momentum is a constant shift, as would be expected from changing the strength of a regulated (smeared) delta function in coordinate space.

A visualization of how two-nucleon interactions evolve in coordinate representation is given for two potentials in the 1S_0 partial wave in Fig. 4, where local projections are applied to the intrinsically non-local SRG evolved potentials [12]. The melting

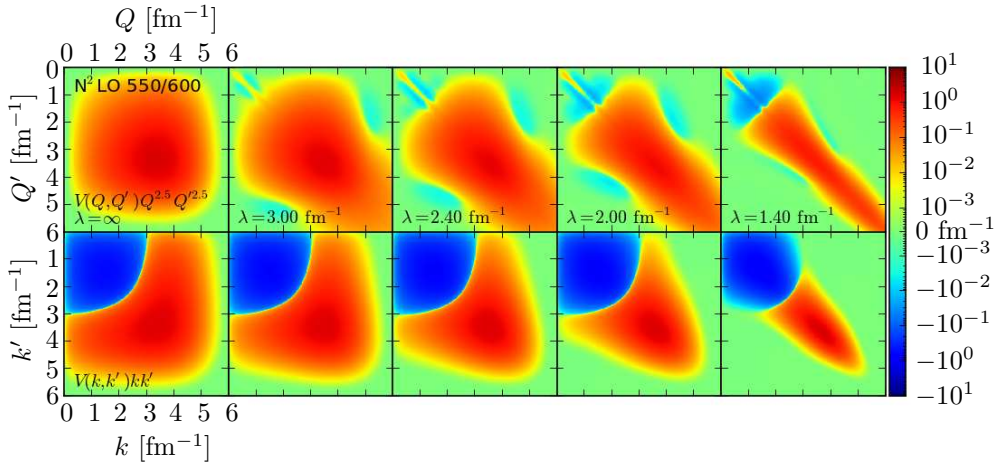


Figure 2: Evolution by the SRG showing flow toward the momentum diagonal for both NN (bottom) and NNN (top) interactions [8]. The initial potential is an $NN + NNN$ chiral EFT interaction at next-to-next-to-leading order (see Ref. [9] for background). λ is a flow parameter with $\hbar^2 \lambda^2 / M$ roughly equal to the energy decoupling scale.

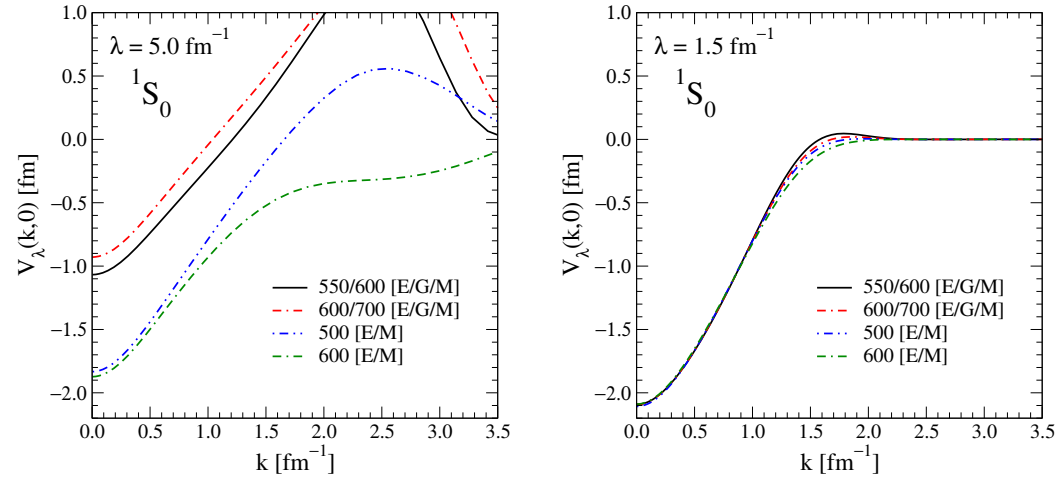


Figure 3: Off-diagonal matrix elements of different chiral EFT potentials evolved by the SRG slightly to $\lambda = 5 \text{ fm}^{-1}$ (left) and much further to $\lambda = 1.5 \text{ fm}^{-1}$ (right) [3].

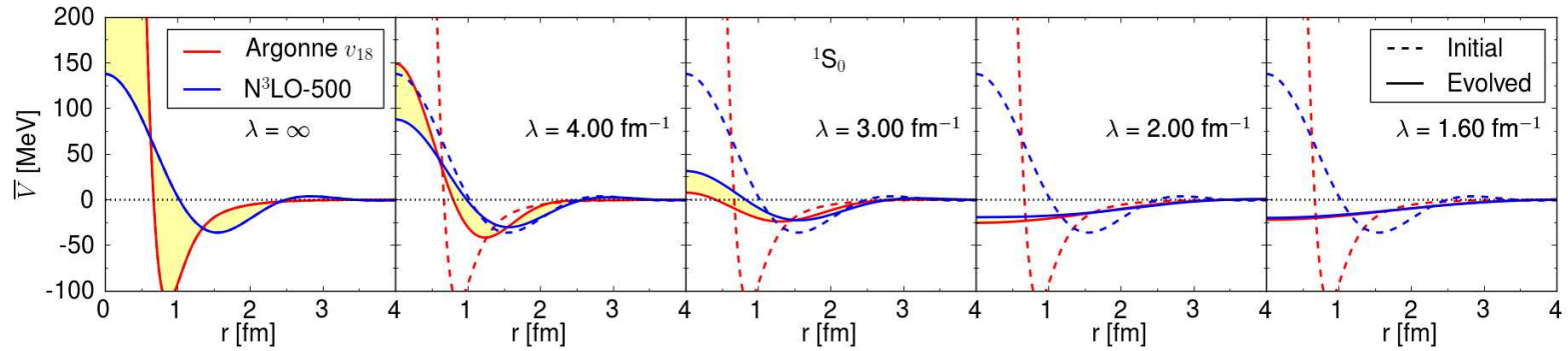


Figure 4: Evolution by the SRG of two NN interactions in coordinate space as visualized by local projections (see Ref. [12] for definitions and details).

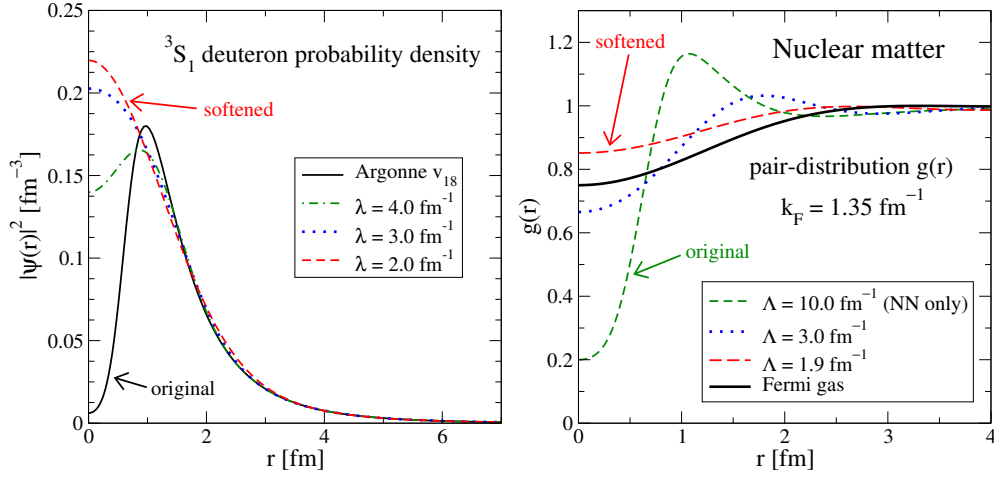


Figure 5: Short-range correlations induced in the $L = 0$ part of the deuteron wave function by the Argonne v_{18} potential [13], seen as a suppression at short distances, is removed with SRG evolution to $\lambda = 2 \text{ fm}^{-1}$ (left). Short-range correlations in nuclear matter, which are manifested by the “wound” in the pair distribution function compared to the Fermi gas, are largely removed by $V_{\text{low } k}$ RG evolution to $\Lambda = 1.9 \text{ fm}^{-1}$ [3].

of the hard repulsive core is manifest as well as the flow to universal form. The soft NN (and NNN) potentials after evolution are much more amenable to many-body methods that use basis expansions, such as the no-core shell model, coupled cluster, and the in-medium SRG (see Ref. [5] for recent results). Indeed, nuclear structure and low-energy reactions are more natural with low-momentum interactions, because the Fermi momentum sets the scale rather than a repulsive core. The successes of this approach with the SRG and other RG methods (e. g., which enable many-body perturbation theory for the shell model) are reviewed elsewhere [3,5]. But because the repulsive core is the dominant source of SRCs, the nuclear wave functions have variable SRCs as the resolution is changed (i. e., as λ is lowered). This is illustrated in Fig. 5 for the deuteron (left) and nuclear matter (right). What then are the implications for RG evolution for the high-resolution (that is, high four-momentum transfer) electron scattering experiments? How does the resolution of the nuclear states even enter the analysis? To address these questions, we must ask about the evolution of operators other than the Hamiltonian.

3 Operator evolution by the SRG

To gain insight into how RG changes in scale should enter the analysis of nuclear knock-out experiments, we can use the extraction of parton distribution functions from deep inelastic scattering (DIS) as a paradigm. The key property that make parton distributions well defined is the controlled factorization of the cross section into structure and reaction parts at hard scales (meaning sufficiently large Q^2) [14]. By this means, a structure function such as $F_2(x, Q^2)$ is decomposed into short-distance physics from the electron-quark scattering that is captured in Wilson coefficients in $\hat{F}_2^a(x, \frac{Q}{\mu_f})$ and the remainder, which is the soft, long-distance physics defining the parton distribution $f_a(x, \mu_f)$ (where a labels quarks):

$$F_2(x, Q^2) \sim \sum_a f_a(x, \mu_f) \otimes \hat{F}_2^a\left(x, \frac{Q}{\mu_f}\right). \quad (1)$$

The *choice* of the factorization scale μ_f defines the border between the long- and short-distance contributions. It is not unique! But because the observable F_2 must be independent of μ_f , knowing how the short-distance part changes with μ_f determines the RG running of the parton distribution. A typical choice is $\mu_f = Q$ (to minimize logarithmic contributions to the Wilson coefficient for the optimal extraction of PDFs from experiment), so this running translates into a Q^2 dependence in the parton distribution [14].

An example of this RG running is shown for the u -quark PDF in a proton as a function of x and Q^2 in Fig. 6. In the top panel, the combination $xu(x, Q^2)$

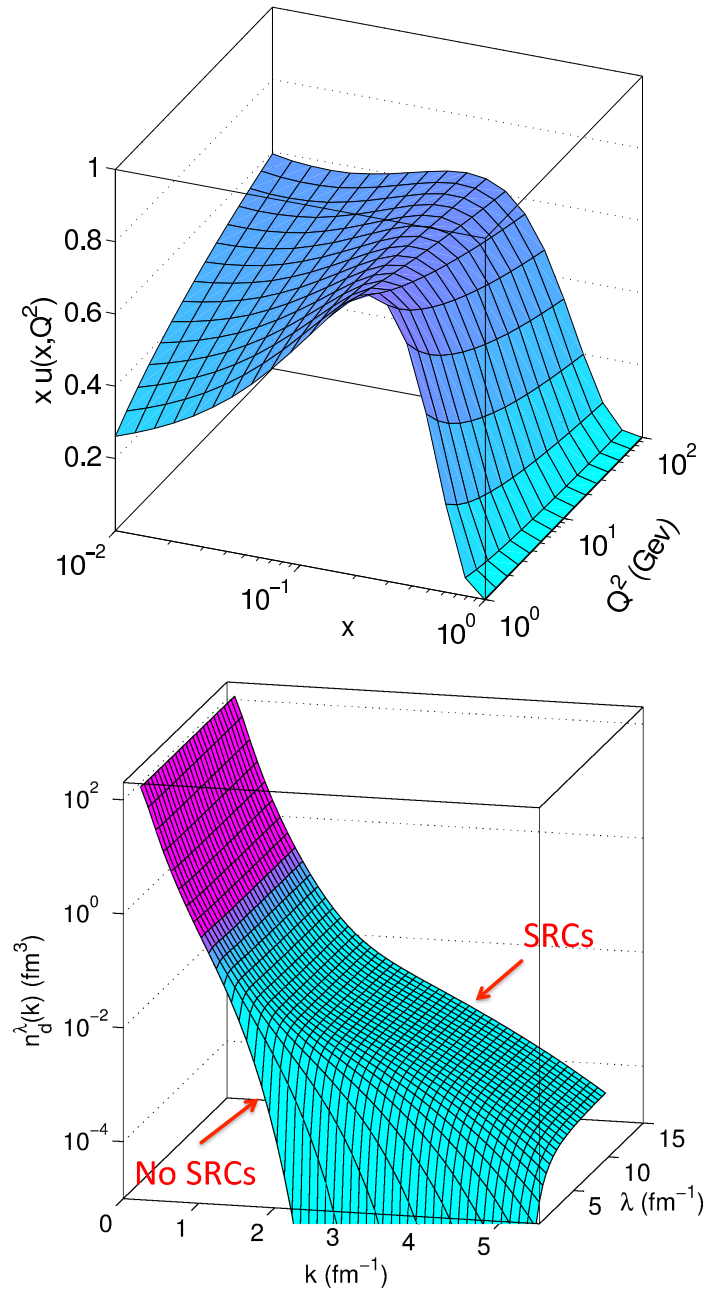


Figure 6: Parton distribution $xu(x, Q^2)$ for the u -quarks in the proton as a function of x and Q^2 (top, calculated from [16]) and deuteron momentum distribution $n_d^\lambda(k)$ at different SRG resolutions λ (bottom).

Again, this means that quantities such as SFs are scale dependent. The bottom line is that the cross section is unchanged only if all pieces are included with the same U : the Hamiltonian, the current operator, and the final state interactions.

Now consider again the high resolution experiment from Fig. 1 and what happens when RG unitary transformations act to change the resolution. In particular, how does the SRC explanation of nuclear scaling, which accounts for plateaus in inclusive cross section ratios, evolve with the resolution scale? This explanation is based on the dominant role played by the one-body current, the two-body interaction, and SRCs.

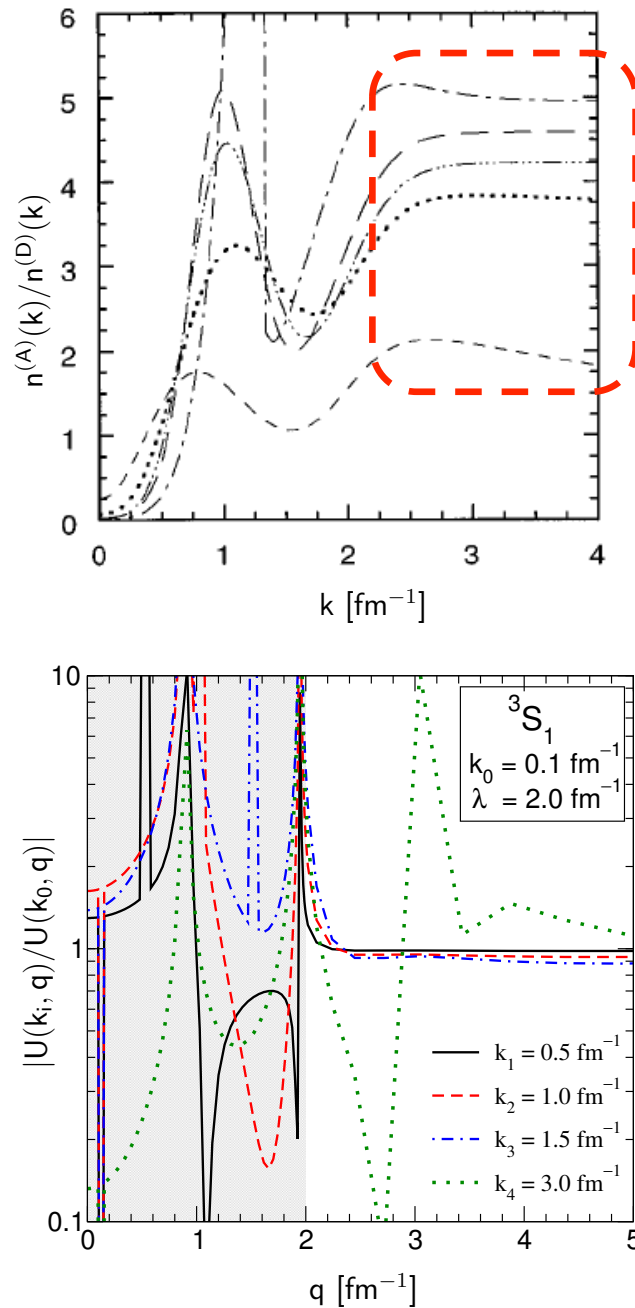


Figure 7: Ratio of momentum distributions in nuclei to the deuteron (denoted n_A and n_d in the text) with a high-resolution potential [17] (top) and U_λ -factorization test for the 3S_1 channel [10] (bottom).

The underlying physics is most simply isolated by considering the high-resolution momentum distributions in nuclei. In Fig. 7 on top, we see that ratios of these momentum distributions in various nuclei to that in the deuteron are almost flat in the high momentum region associated with SRCs (i. e., above $k = 2 \text{ fm}^{-1}$). The contribution highlighted in the circle in Fig. 1 yields a k dependence largely independent of the nuclear environment, so $n_A(k)$ simply scales with A . If we now evolve to lower momentum through unitary transformations, this can no longer explain the cross section, because the softening of the interaction and therefore the wave function means the momentum distribution has no support at these high momenta (e. g., as in Fig. 6 for the deuteron).

But the cross section *must* be unchanged, because it is a unitary transformation. With RG evolution, the probability of high momentum in a nucleus decreases, but if we transform the wave functions *and* operators:

$$n(k) \equiv \langle A | a_{\mathbf{k}}^\dagger a_{\mathbf{k}} | A \rangle = (\langle A | \hat{U}^\dagger) \hat{U} a_{\mathbf{k}}^\dagger a_{\mathbf{k}} \hat{U} (\hat{U} | \Psi_n \rangle) = \langle \tilde{A} | \hat{U} a_{\mathbf{k}}^\dagger a_{\mathbf{k}} \hat{U}^\dagger | \tilde{A} \rangle, \quad (4)$$

then the original momentum distribution is unchanged! We know that the transformed state $|\tilde{A}\rangle$ is easier to calculate, but is the new operator too difficult to calculate or even pathological (e. g., does it explode to compensate for the super-exponential suppression of the low-resolution momentum distribution)?

Let us consider the SRG operator flow for the momentum distribution graphically. The evolution with λ of any operator \hat{O} is given by:

$$\hat{O}_\lambda = \hat{U}_\lambda \hat{O} \hat{U}_\lambda^\dagger, \quad (5)$$

which can be carried out by a flow equation similar to that used to evolve the Hamiltonian. In practice it is more efficient to construct the unitary transformation from $\hat{U}_\lambda = \sum_i |\psi_i(\lambda)\rangle \langle \psi_i(0)|$ or by solving the $dU_\lambda/d\lambda$ flow equation. In any case, matrix elements of evolved operators are unchanged by construction (for the deuteron) *but the distribution of strength flows*. The integrand of the momentum distribution $\langle \psi_d | a_q^\dagger a_q | \psi_d \rangle$ in the deuteron at $q \approx 3.0 \text{ fm}^{-1}$ is shown in Fig. 8. In the top figure, the initial integrand of $\hat{U}_\lambda a_q^\dagger a_q \hat{U}_\lambda^\dagger$ at $\lambda = \infty$ has a delta function at $k = k' = q$. In the

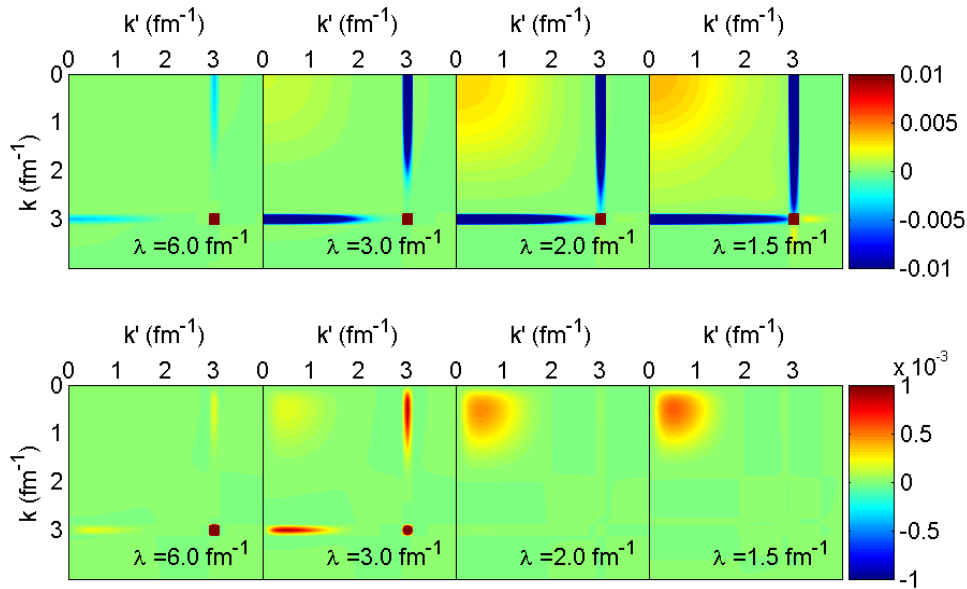


Figure 8: Integrand of the deuteron momentum distribution at $q \approx 3 \text{ fm}^{-1}$ without (top) and with (bottom) the deuteron wave functions included [10].

SRG flow, one-body operators such as $a_q^\dagger a_q$ do not evolve, and their contribution is in fact unchanged with λ . However, there is a clear flow to lower momentum, which must be entirely due to a two-body operator. In the bottom figure, the deuteron wave functions are folded in (such that the integrated area is the invariant value of the original momentum distribution at $q = 3 \text{ fm}^{-1}$). We see there is negligible amplitude at small λ from the original one-body operator (nothing explodes!), but instead a smooth contribution at low momenta from the induced two-body operator, which is reminiscent of a regularized delta function.

We might wish to conclude that this operator flow implies a type of “conservation of difficulty” with the simplification of the wave function countered by the complication of the operator. But in this situation the separation of momentum scales leads to an important generic factorization of the unitary transformation operator U_λ . In particular, U_λ -factorization says that the two-body unitary transformation becomes a simple product (in each partial wave): $U_\lambda(k, q) \rightarrow K_\lambda(k) Q_\lambda(q)$ whenever $k < \lambda$ and $q \gg \lambda$. This result follows from applying effective interaction methods or the operator product expansion (OPE) for nonrelativistic wavefunctions; we refer the reader to Refs. [10, 11] for the technical details. Here we rely on a visual demonstration. In particular, we test U_λ -factorization by considering the ratio of $U_\lambda(k, q)$ at fixed q but variable k . In the factorization region:

$$\frac{U_\lambda(k_i, q)}{U_\lambda(k_0, q)} \xrightarrow[q \gg \lambda]{k < \lambda} \frac{K_\lambda(k_i) Q_\lambda(q)}{K_\lambda(k_0) Q_\lambda(q)} = \frac{K_\lambda(k_i)}{K_\lambda(k_0)} \approx 1, \quad (6)$$

so for $q \gg \lambda$ we expect the ratio to go to a constant, which is in fact unity because $K_\lambda(k)$ becomes independent of k to leading order in the OPE. In Fig. 7 (bottom), we plot this ratio in the 3S_1 channel and see clear plateaus close to one (at the 10–15% level) for those curves with $k_i < \lambda$ in the $q > \lambda$ region, just as expected. It works similarly in other channels [10].

We emphasize that because the leading order for $K_\lambda(k)$ is constant for $k < \lambda$, the factors $K_\lambda(k) K_\lambda(k')$ to good approximation play the role of a contact term. Then the contribution from large λ in the diagram in Fig. 1 (bottom) with an implied integration over q and q' has the simplification:

$$\begin{aligned} \Delta V_\lambda(k, k') &= \int_{q, q'} U_\lambda(k, q) V_\lambda(q, q') U_\lambda^\dagger(q', k') \quad \text{for } k, k' < \lambda, \quad q, q' \gg \lambda \\ &\xrightarrow{U_\lambda \rightarrow K \cdot Q} K(k) \left[\int_{q, q'} Q(q) V_\lambda(q, q') Q(q') \right] K(k') \quad \text{with } K(k) \approx 1, \end{aligned} \quad (7)$$

which is a constant times a smeared delta function, as advertised. Further, we can understand why nuclear scaling is expected directly from U_λ -factorization, if we can argue that the deuteron channel dominates (as in the SRC argument [1, 2]). When $k < \lambda$ and $q \gg \lambda$, the ratio of original momentum distributions becomes (in a schematic notation):

$$\begin{aligned} \frac{n_A(q)}{n_d(q)} &= \frac{\langle \tilde{A} | \tilde{U} a_{\mathbf{q}}^\dagger a_{\mathbf{q}} \tilde{U}^\dagger | \tilde{A} \rangle}{\langle \tilde{d} | \tilde{U} a_{\mathbf{q}}^\dagger a_{\mathbf{q}} \tilde{U}^\dagger | \tilde{d} \rangle} = \frac{\langle \tilde{A} | \int U_\lambda(k', q') \delta_{q'q} U_\lambda^\dagger(q, k) | \tilde{A} \rangle}{\langle \tilde{d} | \int U_\lambda(k', q') \delta_{q'q} U_\lambda^\dagger(q, k) | \tilde{d} \rangle} \\ &= \frac{\langle \tilde{A} | \int K_\lambda(k') [\int Q_\lambda(q') \delta_{q'q} Q_\lambda(q)] K_\lambda(k) | \tilde{A} \rangle}{\langle \tilde{d} | \int K_\lambda(k') [\int Q_\lambda(q') \delta_{q'q} Q_\lambda(q)] K_\lambda(k) | \tilde{d} \rangle} = \frac{\langle \tilde{A} | \int K_\lambda(k') K_\lambda(k) | \tilde{A} \rangle}{\langle \tilde{d} | \int K_\lambda(k') K_\lambda(k) | \tilde{d} \rangle} \\ &\equiv C_A, \end{aligned} \quad (8)$$

where C_A is the scaling ratio. A proof of principle test in a toy one-dimensional model verified that this scenario can work [10]. For the realistic nuclear case, we need to examine all contributions quantitatively, including from three-body operators, but the pattern in Eq. (8) is promising.

We might further speculate that the recent observation that the A dependences of scaling ratios and the slope of the EMC effect $dR_A(x)/dx$ (where $R_A(x)$ is the large Q^2 ratio of nuclear cross sections for $0.7 < x < 1.0$) are linearly correlated [1] could be understood by U_λ -factorization and subsequent cancellations in cross section ratios. The EFT treatment of Chen and Detmold [18] predict an analogous factorization in the EMC ratio. In particular, they assert:

“The x dependence of $R_A(x)$ is governed by short-distance physics, while the overall magnitude (the A dependence) of the EMC effect is governed by long distance matrix elements calculable using traditional nuclear physics.”

If the same leading operators dominate in the two types of processes (i. e., two-body contact operators with deuteron quantum numbers), then we would expect precisely this sort of linear A dependence. Quantitative calculations are needed!

To do such calculations, we need many-body operator contributions, as shown by Neff for ^4He relative momentum distributions [19]. Fortunately, the recently developed technology for evolution of three-body forces can be adopted for more general operator evolution. This will enable direct calculations by *ab initio* methods in lighter nuclei and many-body perturbation theory for operators in heavier nuclei.

4 Summary and outlook

We have presented a brief overview of high-resolution probes of low-resolution nuclei based on the RG/EFT perspective. Some summary observations:

- Lower resolution means more natural nuclear structure.
- While scale and scheme-dependent observables can be (to good approximation) unambiguous for *some* systems, they are often (generally?) not so for nuclei. And while cross sections are invariant, the physics interpretation can change with resolution!
- Working with scale and scheme dependence requires *consistent* Hamiltonian and operators. Be wary of treating experimental analysis in independent pieces (as is often done).
- Unitary transformations can be used to reveal *natural* scheme dependence.

The RG/EFT perspective and associated tools can help to address whether we can have controlled factorization at low energies, to identify the roles of short-range versus long-range correlations, and to quantitatively assess the scheme-dependence of spectroscopic factors and related quantities.

An overreaching question is how should one choose the appropriate scale in different situations (with the RG to evolve the scale as needed). One general motivation is to make calculations easier or more convergent, such as using the QCD running-coupling scale to improve perturbation theory. For nuclear structure and low-energy reactions, low-momentum potentials are chosen to improve convergence in configuration interaction or coupled cluster calculations or to make a microscopic connection to the shell model. Conversely, local potentials (which until recently were only high resolution) are favored for quantum Monte Carlo. The scale could also be chosen for interpretation or intuition; the SRC phenomenology is such an example. But the most important issue for knock-out experiments is to have the cleanest and most controlled extraction of quantities analogous to PDFs from experiment; this might mean optimizing the validity of the impulse approximation but there are other possibilities (e. g., optimizing U_λ -factorization). To make progress, the plan is to make test calculations

with a range of scales starting from initial Hamiltonians and operators matched in an EFT framework, with the RG used to consistently relate scales and quantitatively probe ambiguities (e. g., in spectroscopic factors). A priority calculation in the short term is deuteron electrodisintegration, which is well controlled because of the absence of three-body forces and operators.

I thank my collaborators E. Anderson, S. Bogner, B. Dainton, K. Hebeler, H. Hergert, S. More, R. Perry, A. Schwenk, and K. Wendt. This work was supported in part by the National Science Foundation under Grant No. PHY-1002478 and the U.S. Department of Energy under Grant No. DE-SC0008533 (SciDAC-3/NUCLEI project).

References

- [1] J. Arrington, D. Higinbotham, G. Rosner and M. Sargsian, *Prog. Part. Nucl. Phys.* **67**, 898 (2012).
- [2] M. Alvioli, C. Ciofi degli Atti, L. Kaptari, C. Mezzetti and H. Morita, *Phys. Rev. C* **87**, 034603 (2013).
- [3] S. K. Bogner, R. J. Furnstahl and A. Schwenk, *Prog. Part. Nucl. Phys.* **65**, 94 (2010).
- [4] R. Roth, J. Langhammer, S. Binder and A. Calci, *J. Phys. Conf. Ser.* **403**, 012020 (2012).
- [5] R. Furnstahl and K. Hebeler, *Rep. Prog. Phys.* (*in press*); [arXiv:1305.3800].
- [6] A. H. Guth, K. Huang and R. L. Jaffe, editors, *Asymptotic Realms of Physics*. MIT Press, Cambridge, MA, 1983.
- [7] K. Hebeler, *Phys. Rev. C* **85**, 021002 (2012).
- [8] K. A. Wendt, *Phys. Rev. C* **87**, 061001 (2013).
- [9] E. Epelbaum, H.-W. Hammer and U.-G. Meißner, *Rev. Mod. Phys.* **81**, 1773 (2009).
- [10] E. Anderson, S. Bogner, R. Furnstahl and R. Perry, *Phys. Rev. C* **82**, 054001 (2010).
- [11] S. Bogner and D. Roscher, *Phys. Rev. C* **86**, 064304 (2012).
- [12] K. Wendt, R. Furnstahl and S. Ramanan, *Phys. Rev. C* **86**, 014003 (2012).
- [13] R. B. Wiringa, V. G. J. Stoks and R. Schiavilla, *Phys. Rev. C* **51**, 38 (1995).
- [14] CTEQ Collaboration, R. Brock *et al.*, *Rev. Mod. Phys.* **67**, 157 (1995).
- [15] B. Povh, K. Rith, C. Scholz and F. Zetsche, *Particles and nuclei: an introduction to the physical concepts, 4th ed.* Springer, Berlin, 2004.
- [16] CTEQ Collaboration, H. Lai *et al.*, *Eur. Phys. J. C* **12**, 375 (2000).
- [17] C. Ciofi degli Atti and S. Simula, *Phys. Rev. C* **53**, 1689 (1996).
- [18] J.-W. Chen and W. Detmold, *Phys. Lett. B* **625**, 165 (2005).
- [19] T. Neff, *private communication*.